[15] J. Nanbo, F. Mingya, and Z. Xuexia, "L-band circular polarization microstrip antenna based on the narrow-slot fractal method," in *Proc. IEEE Antennas and Propagation Society Int. Symp.*, 2003, vol. 4, pp. 258–261.
[16] C. Hong-Qi, T. Li-Bin, and H. Bin-Jie, "Compact circularly polarized square microstrip fractal antenna with symmetrical t-slits," in *Proc. Int. Conf. on Wireless Communications, Networking and Mobile Computing*, 2007, pp. 613–616.
[17] F. Congedo, G. Monti, and L. Tarricone, "Broadband bowtie antenna for RF energy scavenging applications," presented at the 4th Eur. Conf. on Antennas and Propag., 2011.
[18] G. Monti and F. Congedo, "UHF rectenna using a bowtie antenna," *Progr. Electromagn. Res. C*, vol. 26, pp. 181–192, 2012.
[19] G. Monti, F. Congedo, D. De Donno, and L. Tarricone, "Monopole-based rectenna for microwave energy harvesting of UHF RFID systems," *Progr. Electromagn. Res. C*, vol. 31, pp. 109–121, 2012.

A Wearable Wideband Circularly Polarized Textile Antenna for Effective Power Transmission on a Wirelessly-Powered Sensor Platform

K. W. Lui, O. H. Murphy, and C. Toumazou

***Abstract*—In this communication, the simulation and experimental results of a novel wideband wearable circularly polarized textile antenna for low-power transmission in the 2.45 GHz ISM band are presented. The wide impedance and axial ratio bandwidths make it perfect for low microwave power transmission to a wearable sensor system. The antenna is flexible, robust and light weight so that it can be easily integrated into clothes. It is shown that the circularly polarized textile antenna has a 3-dB axial ratio bandwidth of 564 MHz (23%) and a −10 dB impedance bandwidth of 1086 MHz (44%) on a human body with the maximum gain of 4.9 dBic. Lastly, the textile antenna is employed on the battery-less temperature sensor system on a human arm to demonstrate the effective power transmission over a metre distance.**

***Index Terms*—Broadband antenna, circular polarization, energy harvesting, ISM band, textile antennas, wireless temperature sensor.**

I. Introduction

Recently there has been growing use of textile antennas for body-centric applications such as healthcare, GPS and fire fighter personal communications [1], [2]. Both linearly and circularly polarized textile antennas are studied. A textile antenna is chosen for such applications due to its lightweight and easy integration into human clothing. However, literature on the simulation of body-worn textile antennas for far-field power harvesting and transmission is rarely found [3].

An antenna with circular polarization is preferred over linear polarization for power transmission due to its independence of orientation. In order for a patch antenna to generate circular polarization, modifications are needed such as cutting a notch at the opposite corners or providing 90° out phase feedings at orthogonal edges [2], [4], [5], but such methods are either complicated or only able to produce circular polarization at a very limited bandwidth without covering the whole 2.45 GHz ISM band [2]. Moreover, due to bending, proximity of the human body and the narrow bandwidth of a patch antenna, the resonant frequency may be shifted due to the movement of a human body or manufacturing variations. As a result, the efficiency of power transmission is degraded at the desired frequency.

In recent years, several high performance wide-slot circularly polarized antennas have been proposed [6], [7]. A coplanar waveguide (CPW) fed antenna features wide impedance and axial ratio bandwidths that are essential to body-worn textile antenna applications as it has higher tolerance to different conditions on a human body. Also it only consists of a single layer of metal. Therefore, a cost effective and high performance body-worn textile antenna can be designed based on a wide-slot antenna topology. However, due to the missing ground plane, the influence of human body to the antenna near field has to be carefully simulated in Microwave Office to ensure the effectiveness of operation. Also the antenna structure has to be simple and robust enough for bending on a human arm and the antenna is able to operate at various distances from a human body.

In this communication, a novel body-worn circularly polarized textile antenna for power transmission of a wirelessly-powered sensor system is presented. The antenna has a −10 dB impedance band covering the 2.45 GHz ISM band (2.4 GHz–2.5 GHz) and is still able to maintain good axial ratio over that band.

Finally the textile antenna is bent to fit on a human arm and is connected to the wirelessly-powered temperature sensor system, the design of which was presented in a previous work [8]. It is shown that the system is able to communicate to a laptop 1.7 meters away with only 50 mW power transmitted from a base station using a helix antenna in an anechoic chamber.

II. Antenna Design

A. Textile Materials and Manufacturing

A planar textile antenna consists of 2 layers as shown in Fig. 1. The top layer is the conductive fabric and the bottom layer is the felt substrate. Both materials have to be highly flexible but also rigid enough to conform on any surface of a human body. A Flectron™ self-adhesive EMI shielding sheet has been chosen for this purpose due to its flexibility and high conductivity ($\leq 0.070\ \Omega/^2$). It is made of a thin metal coating of nickel on non-woven fabrics and can be easily cut without a special tool [9]. A common 1 mm-thick 100% acrylic self-adhesive felt is chosen as the substrate for the antenna due to its flexibility and easy stacking for different thicknesses. The dielectric constant and loss tangent are determined as 1.5 and 0.02, respectively by matching the resonant frequencies of a simple patch antenna from the experimental and simulation results. The antenna is hand-made by cutting along the antenna pattern on the back of the shielding sheet and sticking on a 76×76 mm^2 felt. An end-launch SMA connector is press-fit to the antenna by clamping the feet together and then the conductive silver epoxy is applied to further secure the connection as shown in Fig. 1. The gap between the feed line and the ground is 0.7 mm for easier hand-cutting and so the input impedance is 75 Ω at free space due to the relatively large gap in the feed.

B. Antenna Topology and Simulation

The antenna design objective is to have a wearable antenna to deliver robust low-power transmission to a human body covering the 2.45 GHz ISM band. In order for easy integration into clothing, the textile antenna has to be flexible and 2-dimensional and has a wide impedance

Manuscript received January 29, 2013; accepted March 18, 2013. Date of publication March 27, 2013; date of current version July 01, 2013.

The authors are with the Department of Electrical and Electronic Engineering, Imperial College, South Kensington Campus, London SW7 2AZ, U.K. (e-mail: (k.lui09@imperial.ac.uk).

Color versions of one or more of the figures in this communication are available online at http://ieeexplore.ieee.org.

Digital Object Identifier 10.1109/TAP.2013.2255094

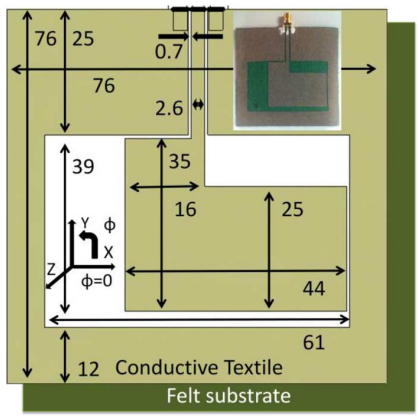

Fig. 1. Textile antenna planar structure with dimensions in mm.

TABLE I
THE CHARACTERISTICS OF HUMAN TISSUES AT 2.45 GHz [11]

Tissue	Thickness (mm)	Conductivity (S/m)	Relative permittivity	Loss Tangent
Skin	3	1.46	38	0.28
Fat	10	0.11	5.28	0.15
Bone	30	0.81	18.5	0.32
Muscle	50	1.73	52.7	0.017

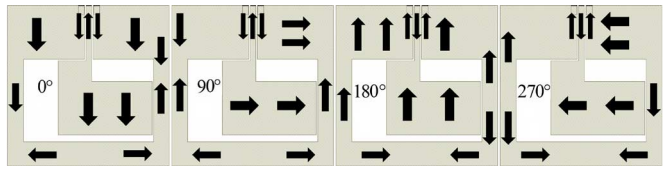

Fig. 2. The simulated current distributions at different phases at 2.45 GHz.

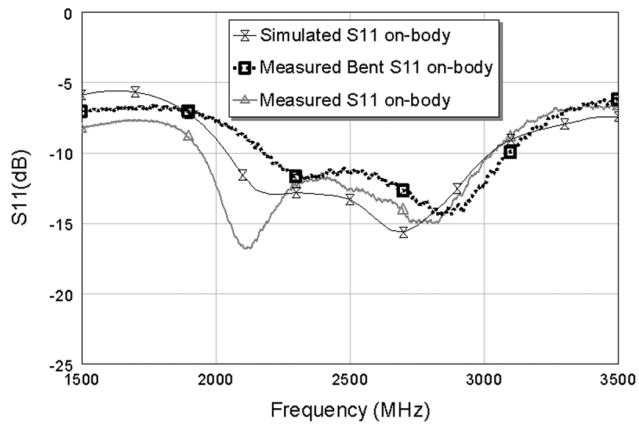

Fig. 3. The measured and simulated S_{11} of the textile antenna.

bandwidth to guarantee that any shift in the resonant frequency due to bending is still within the 2.45 GHz ISM band.

Therefore, a CPW is chosen over a coupling line for feeding because this simplifies the design by using only 1 layer of conductive material without an extra layer. The L-shaped feed line produces the necessary x and y components of magnetic current for circular polarization. The orientation of the bending controls the direction of the circular polarization and RHCP is chosen in this context. The approximate resonant frequency can be estimated by the slightly modified equations [10]:

$$f_r \approx \frac{300}{(L+W)\sqrt{\varepsilon_{r,eff}}}, \quad \varepsilon_{r,eff} = \frac{2\varepsilon_r}{1+\varepsilon_r}. \tag{1}$$

In this empirical formula, f_r is the resonant frequency of the fundamental mode in GHz, L and W are the inner width and length of the slot, respectively in millimeters and $\varepsilon_{r,eff}$ is the effective dielectric constant.

The design process employed here is similar to the one in [6] and it will be briefly described here. The formula (1) is used to establish the initial size of the antenna. Then, a simple constant width L-shaped feed is used to generate the circular polarization. Although the L-shaped feed antenna delivers decent axial ratio bandwidth, the input impedance matching is poor due to the low input reactance and resistance. The improvement can be done by widening the L-shaped feed as suggested. The optimum size of the ground and the dimension of the L-shaped feed line are further experimentally tuned in Microwave Office. As the design is implemented on a flexible textile and not on a circuit board, the geometry cannot be too small as it is difficult to make accurately by hand and more importantly it may be shorted due to bending and so any spacing has to be big enough to accommodate these factors.

The design is firstly simulated without a human body to ensure the modeling is consistent with the measured results. The design process is then repeated with the effect of skin, fat, muscle and bone incorporated in the simulation model with the dielectric constants shown in Table I [11]. The thicknesses of each tissue layer are experimentally tuned and are summarized in Table I. It is also found that the distance between the antenna and human body can significantly affect the performance and the detail will be discussed in the next section. Thickness of the felt substrate is 10 mm for a reasonable performance and is comfortable to wear.

The current distribution of the antenna is simulated and shown in Fig. 2 to understand the mechanism of generating circular polarization. At 0° phase, the majority of current is going downward and at 90° phase, the current turns anticlockwise to right hand side and so on. Therefore, the circular polarization is right handed which is consistent with the experimental results in the next section.

III. EXPERIMENTAL RESULTS

A. Antenna Performance on a Human Body

The simulated and measured on-body S_{11} of the textile antenna are shown in Fig. 3. An Agilent E8361A PNA is used for the S_{11} measurements. The thickness of the substrate and the cotton t-shirt on a human body are 10 mm and 2 mm, respectively. The measured −10 dB impedance bandwidth is 1086 MHz (44%, 1944–3030 MHz) and the simulated impedance bandwidth is 982 MHz (39%, 2042–3024 MHz). The difference between the simulated and measured S_{11} bandwidth can be due to manufacturing error and the variation of dielectric constants of human tissues. The antenna is bent on a human arm with a radius of about 5 cm and it does shift the impedance band (2185–3083 MHz). However, due to the wideband characteristic of the textile antenna, the −10 dB impedance bandwidth is still able to cover the 2.45 GHz ISM band. Therefore, it offers a safe guard band for any shifting in resonant frequency due to bending and variation of dielectric constants of different human bodies.

The axial ratio is an indicator of the quality of circular polarization. The simulated and measured axial ratios at the centre of the textile antenna are shown in Fig. 4. A calibrated double-ridged horn antenna EMC-3115 is used for all the antenna measurements in an anechoic chamber. The simulated and measured 3-dB axial-ratio bandwidths (ARBW) are 502 MHz (21%, 2160–2662 MHz) and 564 MHz (23%,

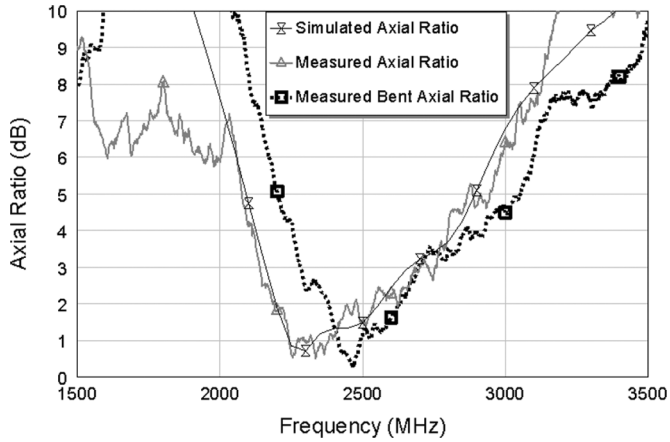

Fig. 4. The measured and simulated axial ratios over frequency.

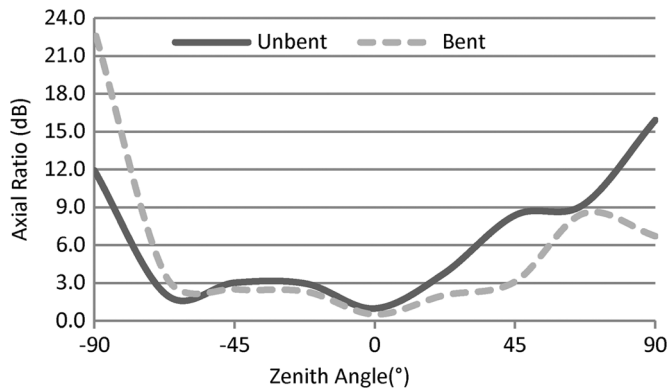

Fig. 5. The measured axial ratios for unbent and bent textile antenna over zenith angle.

2139–2703 MHz) respectively. The difference may be due to the curvature of a human body and mismatch in dielectric constant from the model in the simulation. However, the 3-dB ARBW is still more than enough to cover the 2.45 GHz ISM band with good circular polarization purity and is significantly wider than a standard circularly polarized patch [9]. Bending the textile antenna on a human arm has a small effect on 3-dB ARBW (413 MHz) and has shifted the central frequency slightly higher, but the wide impedance and axial-ratio bandwidths are still maintained on a human body.

The axial ratio versus zenith angle at 2.45 GHz on a human body is shown in Fig. 5. Note that the unbent textile antenna 3-dB and 6-dB axial ratios can cover up to 90° and 110° zenith angles on a human body respectively. Note also that the bent textile antenna is fitted along a human arm and has slightly wider zenith angles for 3-dB and 6-dB axial ratios. The axial ratio distribution is not symmetric around the centre due to its asymmetry in the antenna structure.

The RHCP and LHCP gains versus zenith angles at 2.45 GHz on a human body is shown in Fig. 6. The maximum RHCP gain is 3.5 dBic and is much higher than the LHCP gain as expected and it is consistent with the axial ratio shown in Fig. 4. Note that bending does degrade the centre RHCP gain by 1 dBic, but it still maintains a good purity of RHCP as the LHCP gain is much lower in the centre.

The thickness of the substrate has a significant effect on the textile antenna gain especially as the ground plane is missing because the near field is coupled and absorbed to the body and so the efficiency is decreased as shown in Fig. 7. As the distance between the antenna and a body is increased, the body will behave like a reflector to strengthen the antenna gain [12], [13] and the efficiency is also increased due to less energy loss to the human body as shown in Fig. 7. When the minimum

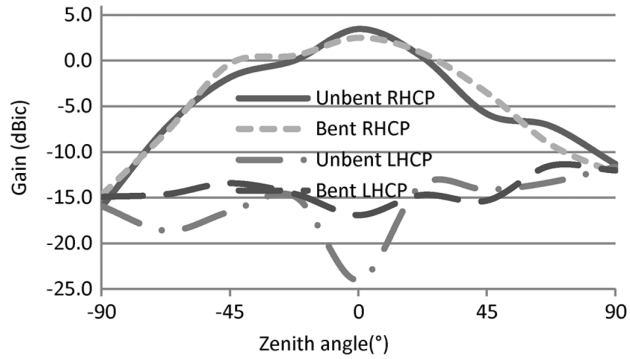

Fig. 6. The measured gains for unbent and bent textile antennas over zenith angle at 2.45 GHz.

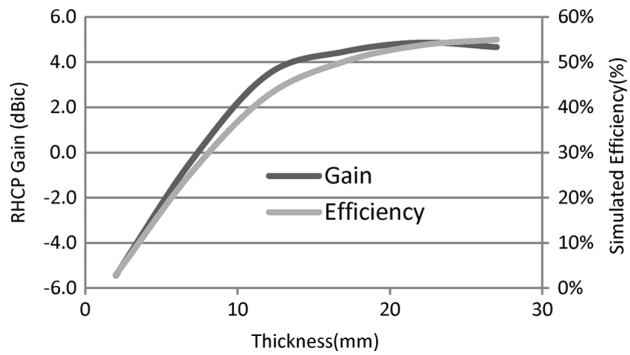

Fig. 7. The RHCP gain and simulated efficiency with variations of the substrate thickness at 2.45 GHz.

distance is at 3 mm (1 mm felt substrate +2 mm of cotton t-shirt), the efficiency is low due to its near field significantly coupled to the human body. However, as the distance increases by inserting the more layers of felt, the gain gradually increases up to maximum 4.9 dBic at the substrate thickness of 22 mm and the gain goes down as the resonant frequency is shifted away from 2.45 GHz. The measured radiation patterns are shown in Fig. 8. In both x-z and y-z planes, good isolation between the LHCP and RHCP gains close to centre is maintained which is consistent with the change in the axial ratio over the zenith angles as shown in Fig. 6.

B. The Transmission Link Between Transponder On-Body and Base Station

Lastly, the textile antenna is attached to the transponder shown in Fig. 9(a) and it is tested on a human body as shown in Fig. 9(b). The detail of the wirelessly-powered sensor system is presented in the previous work [8] A RHCP helix antenna with 12.5 dBic gain is attached to a Rhode & Schwarz signal generator and it can radiate a total of 16.6 dBm (0.046 W) after power losses in the cabling to the anechoic chamber are included. The RF receiver is attached to a logic analyzer for sample recording to the laptop. The longest measured operational distance is 1.74 meters and it is comparable to the previous work with the linearly polarized patch antennas on FR4 without a human body [8].

IV. Conclusion

The design of a wideband circularly polarized textile on-body antenna with a transponder is presented. The design has shown its flexibility in terms of geometry, material, impedance bandwidth and 3-dB ARBW. With a 44% −10 dB impedance bandwidth and a 23% 3-dB ARBW on a human body, it has a huge guard band for manufacturing tolerance and variation on dielectric constants of the different human body. Its structure is simple with only a single conductive layer and a

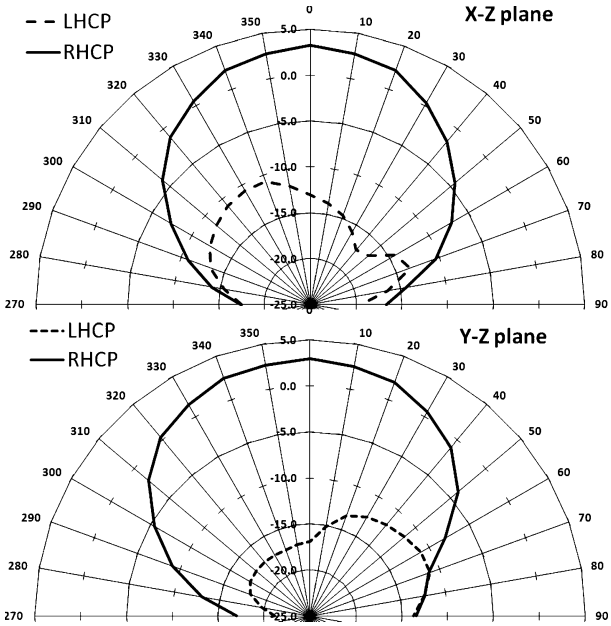

Fig. 8. The measured radiation patterns at 2.45 GHz.

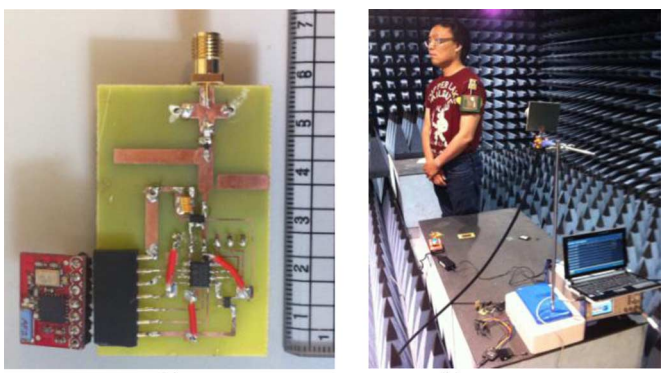

(a) (b)

Fig. 9. (a) The transponder. (b) Testing on a human arm inside the chamber.

single-fed to produce circular polarization. The textile antenna is bent on a human arm with the wirelessly-powered sensor system proved to be operational over a 1.7-meters range with under 0.05 W power transmitted from a base station. This demonstrates that a robust and ultra low-power battery-less μC sensor platform can be implemented and integrated into clothes for other sensing applications in the future.

REFERENCES

[1] E. K. Kaivanto, M. Berg, E. Salonen, and P. de Maagt, "Wearable circularly polarized antenna for personal satellite communication and navigation," *IEEE Trans. Antennas Propag.*, vol. 59, no. 12, pp. 4490–4496, Dec. 2011.

[2] L. Vallozzi, P. Van Torre, C. Hertleer, and H. Rogier, "A textile antenna for off-body communication integrated into protective clothing for firefighters," *IEEE Trans Antennas Propag.*, vol. 57, no. 4, pp. 919–925, Apr. 2009.

[3] D. Masotti, A. Costanzo, and S. Adami, "Design and realization of a wearable multi-frequency RF energy harvesting system," in *Proc. 5th Eur. Conf. Antennas Propag.*, Apr. 11–15, 2011, pp. 517–520.

[4] E. Kaivanto, J. Lilja, M. Berg, E. Salonen, and P. Salonen, "Circularly polarized textile antenna for personal satellite communication," in *Proc. 4th Eur. Conf. Antennas Propag.*, Apr. 12–16, 2010, pp. 1–4.

[5] M. Klemm, I. Locher, and G. Troster, "A novel circularly polarized textile antenna for wearable applications," in *Proc. 7th Eur. Conf. Wireless Tech.*, Oct. 12, 2004, pp. 285–288.

[6] J.-Y. Sze and W.-H. Chen, "Axial-ratio-bandwidth enhancement of a microstrip-line-fed circularly polarized annular-ring slot antenna," *IEEE Trans. Antennas Propag.*, vol. 59, no. 7, pp. 2450–2456, Jul. 2011.

[7] J.-Y. Sze, C.-I. G. Hsu, Z.-W. Chen, and C.-C. Chang, "Broadband CPW-Fed circularly polarized square slot antenna with lightening-shaped feedline and inverted-L grounded strips," *IEEE Trans. Antennas Propag.*, vol. 58, no. 3, pp. 973–977, Mar. 2010.

[8] K. W. Lui, O. H. Murphy, and C. Toumazou, "32 μW wirelessly-powered sensor platform with a 2-m range," *IEEE Sensors J.*, vol. 12, no. 6, pp. 1919–1924, Jun. 2012.

[9] "EMI Flectron Metallized Fabrics Specification Sheet," Lairtech Technologies, 1998.

[10] C. C. Chou, K. H. Lin, and H. L. Su, "Broadband circularly polarised crosspatch-loaded square slot antenna," *Electron. Lett.*, vol. 43, no. 9, pp. 485–486, Apr. 26, 2007.

[11] R. Fossi, C. Petrucci, and D. Andreuccetti, Calculation of the Dielectric Properties of Body Tissues in the Frequency Range 10 Hz–100 GHz [Online]. Available: http://niremf.ifac.cnr.it/tissprop/ 1997

[12] M. Klemm and G. Troester, "Textile UWB antennas for wireless body area networks," *IEEE Trans. Antenna Propag.*, vol. 54, no. 11, pp. 3192–3197, Nov. 2006.

[13] H. Giddens, D. L. Paul, G. S. Hilton, and J. P. McGeehan, "Influence of body proximity on the efficiency of a wearable textile patch antenna," in *Proc. 6th Eur. Conf. Antennas Propag.*, Mar. 26–30, 2012, pp. 1353–1357.

A Dual Band Leaky Wave Antenna on a CRLH Substrate Integrated Waveguide

Jan Machac, Milan Polivka, and Kirill Zemlyakov

***Abstract*—This communication presents the results of an investigation of a new version of a leaky wave antenna designed on a CRLH substrate integrated waveguide. The antenna operates in two frequency bands and its main beam can be steered from backward to forward direction by changing the frequency. The antenna structure is planar and can be fabricated by a standard PCB technology, so it is suitable for mass production. An efficient method for determining the complex dispersion characteristic of periodic 1D structure is proposed.**

***Index Terms*—Composite right/left-handed transmission line, leaky wave antenna, substrate integrated waveguide.**

I. INTRODUCTION

Low profile planar antennas can be integrated with other circuits and can be easily fabricated. They are therefore suitable for cheap mass production. They have been of great interest to researchers and designers

Manuscript received November 01, 2012; revised February 10, 2013; accepted March 16, 2013. Date of publication April 02, 2013; date of current version July 01, 2013. This work was supported by the Grant Agency of the Czech Republic under the project 13-09086S, and by the Czech Technical University in Prague under the project OHK3-011/13.

J. Machac and M. Polivka are with the Department of Electromagnetic Field, Technical University in Prague, 16627 Praha 6, Czech Republic (e-mail: polivka@fel.cvut.cz; machac@fel.cvut.cz).

K. Zemlyakov is with St. Petersburg Electrotechnical University, 197376 St. Petersburg, Russia (e-mail: kirill.zemlyakov@gmail.com).

Color versions of one or more of the figures in this communication are available online at http://ieeexplore.ieee.org.

Digital Object Identifier 10.1109/TAP.2013.2256097